CFD Based Aeroelastic Stability Predictions Under the Influence of Structural Variability

S.Marques[*], K.J. Badcock [†], H.H. Khodaparast[‡] and J.E.Mottershead[§]

Department of Engineering,

University of Liverpool,

L69 3BX, United Kingdom.

Flutter prediction as currently practised is almost always deterministic in nature, based on a single structural model that is assumed to represent a fleet of aircraft. However, it is also recognised that there can be significant variability, even for different flights of the same aircraft. The safety factor used during flutter clearance is in part meant to account for this variability. Simulation tools can however represent the consequences of structural variability in the flutter predictions, providing extra information which could be useful in planning physical tests and assessing risk. The main problem arising for this type of calculation when using high fidelity tools based on Computational Fluid Dynamics (CFD) is the computational cost. The current paper uses an eigenvalue based stability method together with CFD level aerodynamics and different methods for propagating structural variability to stability predictions. The propagation methods are Monte Carlo, perturbation and interval analysis. The feasibility of this type of analysis is demonstrated. Results are presented for the Goland wing and for a generic fighter configuration.

I. NOMENCLATURE

Symbols

A	Jacobian matrix
b	optimisation problem constraints
d	optimisation search direction
E	Young's modulus of elasticity
g and G	the first and second Jacobians of γ_i with respect to θ
G	shear modulus
H	optimisation objective function Hessian
I	moment of inertia
$\mathcal{L}$	Lagrangian
m_i^r	the rth statistical moment of γ_i with respect to the θ
p	eigenvector
q	Lagrangian approximate quadratic approximate function
R	Residual vector of the fluid and/or structural model
S	Schur complement matrix
t	thickness
w	vector of fluid and/or structural unknowns
Var	Variance

Greek

[*]Research Assistant

[†]Professor, SMAIAA, corresponding author. Tel. : +44(0)151 794 4847 , Fax. : +44(0)151 794 6841, Email : K.J.Badcock@liverpool.ac.uk

[‡]Research Assistant

[§]Professor

American Institute of Aeronautics and Astronautics

γ_i	either the real or imaginary part of an aeroelastic eigenvalue
λ	eigenvalue
μ	Bifurcation parameter (altitude)
φ	Lagrangian multiplier vector
θ	m-dimensional vector containing the m uncertain structural parameters

Subscripts or superscripts

f	fluid model
s	structural model
0	equilibrium
xx, yy, zz	axis for moment of inertia
$\overline{\theta}$	the mean value of θ

II. <u>Introduction</u>

An important area of research is how to account for variability in aeroelastic[1] and aerodynamic analysis.[2] Uncertainty can be classified into two different categories.[1] Aleatory uncertainty includes randomness in parameters. Epistemic uncertainty includes limitations in knowledge or lack of understanding, and uncertainty due to human error. Several methodologies have been developed to introduce the effects of uncertainty into design procedures or engineering analysis. Two popular classes of methods have emerged:[2] probabilistic methods include Monte-Carlo, moment methods and polynomial chaos. Non-probabilistic methods include interval analysis and error propagation with sensitivity derivatives. The focus of this paper is to consider how uncertainty in structural parameters can be efficiently propagated to aeroelastic stability predictions when expensive CFD level aerodynamics is used.

Structural variability arises from a variety of sources, such as manufacturing tolerances, material differences and wear. A study of the McDonnell Douglas F-4 Phantom II[3] quantified the weight and inertia variability for this aircraft, showing changes in mass and stiffness properties of up to 15%. Quantifying uncertainty has been a subject of interest in the structures community for several years and numerous methods have been used.[4,5]

In this work, the critical structural parameters from an aeroelastic stability viewpoint are first identified, and then an estimate of the possible distribution or range of these parameters is made. This variability can then be propagated to a distribution in the flutter speed through an analysis code. This approach was previously taken for the Goland wing[6] with linear analysis used to compute the flutter speed. This is computationally efficient since the aerodynamic matrices can be pre-computed and then used for all normal mode sets arising from the varying structural parameters. The probability density functions for the flutter speeds were computed, and some critical cases identified which were then recomputed using a time domain transonic small disturbance code. Wilcox and Peraire,[7] applied a two-dimensional time domain Euler CFD code to assess the variability in frequencies of bladed disks and the effects in the tuning of cascades. Blade structural variability was translated in a frequency probability density function (pdf) and the coupled aeroelastic system was solved making use of reduced order model (ROM) methods. Verhoosel[8] used a monolithic fluid-structure interaction (FSI) code to model panel flutter under the presence of variability in the Young's modulus. In this case, the fluid flow was described by a two-dimensional unsteady linearised potential equation, and the structure was modelled by the Euler-Bernoulli beam equation. The parameter variability was represented by a Gaussian distribution obtained from a Karhunen - Loeve expansion and applied to perturbation methods. Rao and Majunder[9] applied interval analysis to a structural optimisation problem under atmospheric uncertainty. Interval analysis finds the upper and lower extremes for possible response to parameteric variation. The parameters were allowed to deviate $\pm 0.5\%$ from the nominal values. The structure was optimised for a gust response with constraints on flutter Mach number, weight and energy. The authors concluded that interval analysis provides comparable results to probabilistic methods and should be used where probability distributions are difficult to obtain.

An extra difficulty is introduced when CFD level aerodynamics is used for the aeroelastic analysis, namely the computational cost. Methods have been under development to reduce

the cost of computing transonic flutter speeds using CFD methods for the aerodynamics.[10] These methods provide a suitable framework for doing analysis for the effects of stuctural variability since they operate on the aeroelastic modes. The modes of interest can be identified and analysed for dependence on the uncertain structural parameters. There are several ways in which this can be done including the Monte-Carlo method, perturbation methods and interval analysis.

The purpose of this paper is to investigate the practicality of using CFD derived aerodynamics for variability analysis of aeroelastic stability. The stability and variability propagation methods are described and then results are presented for the Monte-Carlo method, perturbation methods and interval analysis applied to the Goland wing and a generic fighter. The emphasis is placed on demonstrating that eigenvalue based stability calculations (with CFD level aerodynamics) are computationally efficient enough to allow the variability analysis.

III. Aeroelastic Stability Formulation

The semi-discrete form of the coupled CFD-FEM system is written as

$$\frac{d\mathbf{w}}{dt} = \mathbf{R}(\mathbf{w}, \mu) \tag{1}$$

where

$$\mathbf{w} = [\mathbf{w}_f, \mathbf{w}_s]^T \tag{2}$$

is a vector containing the fluid unknowns ($\mathbf{w}_f$) and the structural unknowns ($\mathbf{w}_s$), and

$$\mathbf{R} = [\mathbf{R}_f, \mathbf{R}_s]^T \tag{3}$$

is a vector containing the fluid residual ($\mathbf{R}_f$) and the structural residual ($\mathbf{R}_s$). The residual also depends on a parameter μ (in this paper μ is altitude) which is independent of $\mathbf{w}$. An equilibrium $\mathbf{w}_0(\mu)$ of this system satisfies $\mathbf{R}(\mathbf{w}_0, \mu) = \mathbf{0}$.

The stability of equilibria of equation 1 is determined by eigenvalues of the Jacobian matrix $A = \partial \mathbf{R}/\partial \mathbf{w}$. In the current work a linear stability analysis is done based on the coupled system Jacobian matrix which includes the Jacobian of the CFD residual with respect to the CFD and structural unknowns. The calculation of the Jacobian A is most conveniently done by partitioning the matrix as

$$A = \begin{bmatrix} \frac{\partial \mathbf{R}_f}{\partial \mathbf{w}_f} & \frac{\partial \mathbf{R}_f}{\partial \mathbf{w}_s} \\ \frac{\partial \mathbf{R}_s}{\partial \mathbf{w}_f} & \frac{\partial \mathbf{R}_s}{\partial \mathbf{w}_s} \end{bmatrix} = \begin{bmatrix} A_{ff} & A_{fs} \\ A_{sf} & A_{ss} \end{bmatrix}. \tag{4}$$

The details of the Jacobian calculation are given in references[11] and.[12]

In the current work, and as is conventional in aircraft aeroelasticity, the structure is modelled by a small number of modes, and so the number of the fluid unknowns is far higher than the structural unknowns. This means that the Jacobian matrix has a large, but sparse, block A_{ff} surrounded by thin strips for A_{fs} and A_{sf}. As described in reference[10] the stability calculation is formulated as an eigenvalue problem, focussing on eigenvalues of the coupled system that originate from the uncoupled block A_{ss}.

Write the coupled system eigenvalue problem as

$$\begin{bmatrix} A_{ff} & A_{fs} \\ A_{sf} & A_{ss} \end{bmatrix} \mathbf{p} = \lambda \mathbf{p} \tag{5}$$

where $\mathbf{p}$ and λ are the complex eigenvector and eigenvalue respectively. Partition the eigenvector as

$$\mathbf{p} = [\mathbf{p}_f, \mathbf{p}_s].^T \tag{6}$$

The eigenvalue λ (assuming it is not an eigenvalue of A_{ff}) satisfies[13] the nonlinear eigenvalue problem

$$S(\lambda)\mathbf{p}_s = \lambda \mathbf{p}_s \tag{7}$$

where $S(\lambda) = A_{ss} - A_{sf}(A_{ff} - \lambda I)^{-1} A_{fs}$.

The nonlinear equation 7 is solved using Newton's method. Each iteration requires the formation of the residual, $S(\lambda)\mathbf{p}_s - \lambda \mathbf{p}_s$ and its Jacobian matrix. The calculation of the

American Institute of Aeronautics and Astronautics

correction matrix, $A_{sf}(A_{ff} - \lambda I)^{-1}A_{fs}$, is required to form the Jacobian matrix. This can be achieved through $2n$ solutions of a linear system against $A_{ff} - \lambda I$, one for each column of A_{fs}. These solutions are then multiplied against A_{sf}. Now, for each value of the bifurcation parameter, there are n solutions of the nonlinear system in equation 7, and so the cost of forming the correction matrix at each Newton step, for each solution and for a range of parameters becomes too high. To overcome this the expansion

$$(A_{ff} - \lambda I)^{-1} = A_{ff}^{-1} + \lambda A_{ff}^{-1}A_{ff}^{-1} + \lambda^2 A_{ff}^{-1}A_{ff}^{-1}A_{ff}^{-1} + \ldots \tag{8}$$

is used where λ must be small for the series to converge. Note that this restriction can be overcome by assuming that the eigenvalue we are calculating is a small change from the eigenvalue λ_0 of A_{ss}. Then λ_0 can be used as a shift to the full system eigenvalue problem by replacing A_{ff} by $A_{ff} - \lambda_0 I$ and A_{ss} by $A_{ss} - \lambda_0$. This modifies the nonlinear eigenvalue problem in equation 7 by redefining $S(\lambda) = (A_{ss} - \lambda_0 I) - A_{sf}(A_{ff} - \lambda_0 I - \lambda I)^{-1}A_{fs}$. The series approximation then becomes

$$(A_{ff} - \lambda_0 I - \lambda I)^{-1} = (A_{ff} - \lambda_0 I)^{-1} + \lambda(A_{ff} - \lambda_0 I)^{-2} + \lambda^2(A_{ff} - \lambda_0 I)^{-3} + \ldots \tag{9}$$

where λ is a small change to λ_0. When the nonlinear eigenvalue problem is solved for λ, the eigenvalue of the original system is then $\lambda_0 + \lambda$.

This method is referred to as the Schur method. Two forms are available. In both cases the series approximation is used for approximating the Jacobian matrix of the residual from equation 7. For the residual the evaluation of $S(\lambda)\mathbf{p}_s - \lambda\mathbf{p}_s$ can be made based on an exact evaluation (referred to as *full* in this paper) which requires the solution of one linear system against $A_{fs}\mathbf{p}_s$, or can use the series approximation (referred to as *series*) at virtually no additional cost after the series matrices are formed.

IV.   Variability Formulation

A.   Eigenvalue Calculations

In this paper we assume that the values of some structural parameters θ are uncertain, defined either through a probability density function or by an interval of equally possible values. In either case we can define a mean or midpoint value. The building block for the propagation of the uncertainty in the structural parameters to the uncertainty in the aeroelastic eigenvalues is the ability to evaluate the eigenvalue at low cost for any desired value of the parameter vector θ. This is done in the following way. The matrices for the series approximation in equation 8 are first evaluated at the mean or midpoint value for θ. This series approximation is then used to drive the Newton convergence to the aeroelastic eigenvalues for any mode set derived from the required value of θ. The residual $S(\lambda)\mathbf{p}_s - \lambda\mathbf{p}_s$ must be evaluated using the full evaluation since the series approximation is only valid for the mean or midpoint structural parameters. In this way the aeroelastic eigenvalue for a modified mode set can be obtained in a small number of additional linear solves once the mean parameter series approximation to S is calculated. This approach is at the heart of the propagation methods now described.

B.   Monte Carlo Simulation

In a Monte Carlo process a large number of samples of the uncertain structural parameters θ are generated according to the assumed parameter probability density function. In the current work this leads to different normal mode shapes and frequencies which are then used for the aeroelastic calculations. The respective response values, the real and imaginary parts of the aeroelastic eigenvalues, γ_i (which denotes either the real or imaginary part of the ith eigenvalue) are evaluated using the Schur method as described in the previous section. The mean values and standard deviation of the eigenvalues can be directly evaluated from the scatter of the computed values. The continuous probability density function cannot be calculated directly from discrete response samples. Considering the Kernel density function[14] leads to an estimate of the probability density function from a discrete set of samples. The Kernel density estimation can be calculated as a weighted sum of Gaussian pdfs centred around these samples.

American Institute of Aeronautics and Astronautics

C. Statistical moments using theory of quadratic forms

The real and imaginary parts of eigenvalues obtained by the Schur method at a fixed altitude can be expanded about the mean value of the uncertain structural parameters as

$$\gamma_i = \gamma_i(\overline{\theta}) + \mathbf{g}(\theta - \overline{\theta}) + \mathbf{G}(\theta - \overline{\theta})^2 + \dots \tag{10}$$

where $\mathbf{g} = [\partial\gamma_i/\partial\theta]$ is the first Jacobian, and $\mathbf{G} = [\partial^2\gamma_i/\partial\theta_i\partial\theta_k]$ is the second Jacobian, given by

$$\mathbf{G}(\theta - \overline{\theta})^2 = \Sigma_{i=1}^{m}\Sigma_{j=1}^{m}\frac{\partial^2\gamma_i}{\partial\theta_j\partial\theta_k}(\theta_j - \overline{\theta_j})(\theta_k - \overline{\theta_k}) \tag{11}$$

In eq.11 the partial derivatives are evaluated at the mean structural parameters.

According to quadratic theory,[15] the statistical moments of γ_i can be obtained as

$$m_i^1 = \gamma_j(\overline{\theta}) + \frac{1}{2}Trace(\mathbf{G}_{\gamma_i}(\theta)Cov(\theta,\theta)) \tag{12}$$

and, if $r \geq 2$,

$$m_i^r = \frac{r!}{2}\mathbf{g}_{\gamma_i}(\theta)^T[\mathbf{G}_{\gamma_i}(\theta)Cov(\theta,\theta)]^{r-2}Cov(\theta,\theta)\mathbf{g}_{\gamma_i}(\theta) + \frac{(r-1)!}{2}Trace(\mathbf{G}_{\gamma_i}(\theta)Cov(\theta,\theta))^r. \tag{13}$$

The mean $\hat{\gamma}_j$ can be obtained for $r = 1$ (i.e. from equation 12) and the variance $Var(\gamma_j)$ for $r = 2$ as

$$Var(\gamma_j) = \mathbf{g}_{\gamma_i}(\theta)^T Cov(\theta,\theta)\mathbf{g}_{\gamma_i}(\theta) + \frac{1}{2}Trace(\mathbf{G}_{\gamma_i}(\theta)Cov(\theta,\theta))^2. \tag{14}$$

If only first order terms are retained then $\hat{\gamma}_j = \gamma_j(\overline{\theta})$ and $Var(\gamma_j) = \mathbf{g}_{\gamma_i}(\theta)^T Cov(\theta,\theta)\mathbf{g}_{\gamma_i}(\theta)$.

If the statistical moments are known then the probability density function can be derived by the maximum entropy method[16,17] as

$$P(\gamma_i) = \frac{1}{\sqrt{2\pi m_i^{(2)}}}exp\left[-\frac{\overline{\gamma}_i - m_i^{(1)}}{2\pi m_i^{(2)}}\right] \tag{15}$$

where σ_j is the standard deviation derived from the variance.

The first and second Jacobian matrices need to be evaluated at the mean structural parameters to calculate the statistical moments. This is done in two stages. First, normal mode shapes and frequencies are calculated at perturbed values of the structural model parameters. Then, the Schur method is used to evaluate the aeroelastic eigenvalues at the perturbed parameter values. This is done using the Schur matrix already computed at the mean parameter values to drive the convergence of the quasi-Newton iterations for the perturbed mode shapes and frequencies (i.e. the residual function is evaluated for the perturbed mode shapes). For the first Jacobian one nonlinear system needs to be solved for each structural parameter to obtain the Jacobian matrices for the real and imaginary parts of each aeroelastic eigenvalue. For the second Jacobian $m(m-1)$ nonlinear systems must be solved if there are m structural parameters.

D. Interval Analysis

An interval analysis defines a range for the uncertain structural parameters, and then computes the possible range for the aeroelastic eigenvalues. The interval flutter problem is expressed as

$$\begin{cases} [\underline{\lambda}(\theta)_i, \overline{\lambda}(\theta)_i] & = [min(Re(\lambda_i)), max(Re(\lambda_i))] \\ S(\lambda_i)\mathbf{p}_s - \lambda_i\mathbf{p}_s & = 0, \ \forall i \\ \underline{\theta} \leq \theta \leq \overline{\theta} \end{cases} \tag{16}$$

The index i indicates the critical mode, and the under and over bars indicate the lower and upper bounds of the variable. A range for each of the important structural parameters is chosen, and then an optimisation problem must be solved to find the range on the critical eigenvalue. In the current work a minimisation function in Matlab (*fmincon*), that solves a constrained non-linear multivariate problem, is used. This method requires the parameter constraints (i.e. intervals) and a scalar objective function. The computations are performed by a Sequential Quadratic Programming (SQP) method[18–20] to update the estimate of the Hessian of the Lagrangian. The parameter space is explored by a line search.

American Institute of Aeronautics and Astronautics

First order optimality is based on the Karush-Kuhn-Tucker (KKT) conditions. These conditions not only require for gradient to be zero at a minimum, but also consider the problem constraints. The KKT are formulated via an approximate function of the Lagrangian, given by

$$\mathcal{L}(\theta, \varphi) = \lambda(\theta) + \Sigma \varphi_j b_j(\theta) \tag{17}$$

where $\lambda(\theta)$ is the objective function, $b(\theta)$, represents the inequality and equality constraints shown in eq.16 and φ_j is the Langrangian multiplier vector which has dimension equal to the number of constraints. The optimality measure associated with the KKT conditions is

$$\|\nabla_\theta \mathcal{L}(\theta, \varphi)\| = \|\nabla \lambda(\theta) + \Sigma \varphi_j \nabla b_j(\theta)\| \tag{18}$$

At each major iteration, an approximation is made to the Hessian of the Lagrangian function using a quasi-Newton updating method. This is then used to generate a quadratic programming subproblem whose solution is used to form a search direction. The Hessian is updated at each major iteration of the SQP algorithm, using the Broyden, Fletcher, Goldfarb, and Shanno (BFGS) update method. The major computational cost is incurred in calculating the Jacobian of the eigenvalue with respect to the structural parameters, which entails a Schur eigenvalue calculation for each uncertain structural parameter.

V.   Results

A.   Goland Wing

The Goland wing, shown in figure 1, has a chord of 6 feet and a span of 20 feet. It is a rectangular cantilevered wing with a 4% thick parabolic section. The structural model follows the description given in reference,[21] and is shown in figure 1. The CFD grid is block structured and uses an O-O topology. This allows points to be focussed in the tip region which is most critical for the aerodynamic contribution to the aeroelastic response. The fine grid has 236 thousand points and a coarse level was extracted from this grid, which has 35 thousand points. Views of the fine grid are shown in figure 1. Four mode shapes were retained for the aeroelastic simulation. The Schur eigenvalue formulation was evaluated for the Goland wing test case in reference.[10]

The different structural components of the wing are shown in figure 2. It is composed of upper and lower skins, three spars with caps, eleven ribs with caps and 33 posts. There are two versions of the wing which are considered, namely with and without a tip store. The wing without a tip store is referred to as clean. The tip store is added to the clean wing by including a point mass at some streamwise location at the wing tip. The baseline tip mass configuration has the mass located 0.25 ft from the leading edge. In both cases the parameters which define the geometry of the structural model are the thicknesses of the skins, the areas of the spar and rib caps, the thicknesses of the spars and ribs and the areas of the posts. The mean values of these parameters follow those given in reference.[6] It should be noted that the density of the structural elements was taken to be negligible and the inertial properties are modelled as lumped mass elements shown in figure 2(a). As a consequence the mass and stiffness properties of the wing are decoupled.

The sensitivity of the flutter speed for the clean wing to each of the structural parameters was previously calculated using a linear method.[22] This was done to indicate which structural parameters should be considered for the nonlinear analysis. The sensitivity of the aerodynamic damping at Mach 0.5 and sea level with respect to each parameter is shown in figure 3. This shows that there are 7 parameters which are key to determining the flutter speed, namely the thicknesses of the leading and trailing edge spars, the thicknesses of the upper and lower skins, and the areas of the leading edge, trailing edge and centre spar caps. Note that the sensitivities here are with respect to the parameters normalised by their mean value.

B.   Clean Wing Results

The clean wing flutter response was calculated at the mean structural parameters. This was done at Mach 0.5 for matched conditions. At Mach 0.5, an interaction between the wing first bending and torsion modes gives flutter between ground level and 10000 ft. Although no transonic effects are present at this Mach number the CFD based Schur method was

American Institute of Aeronautics and Astronautics
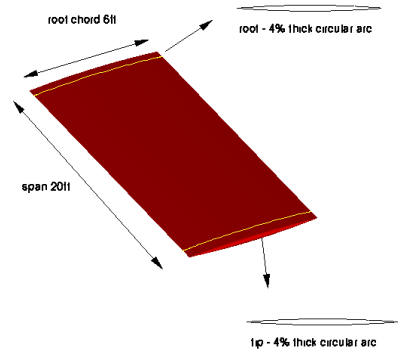
Summary of Geometry
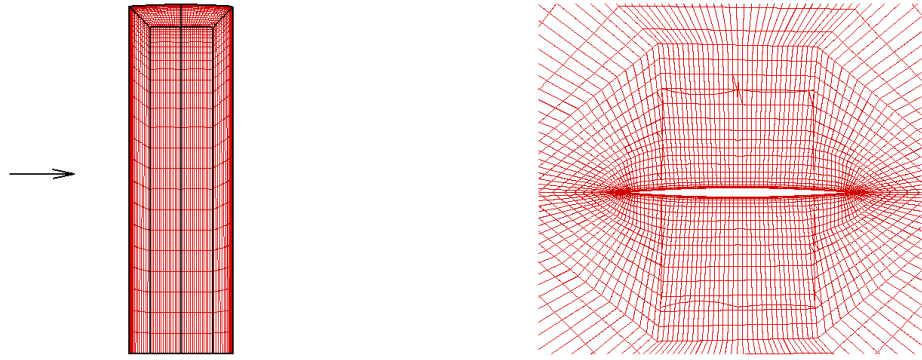
surface CFD grid   slice from volume CFD grid

Figure 1. Views of geometry and CFD Grids for the Goland Wing.[10]

FE Model

Skins

Thicknesses of skins (2 parameters)

Thicknesses of spars (3 parameters)

Spars

Thicknesses of ribs (11 parameters)

Ribs

Area of spars cap (11 parameters)

Spar Caps

Area of ribs cap (11 parameters)

Rib Caps

Area of posts (33 parameters)

Posts
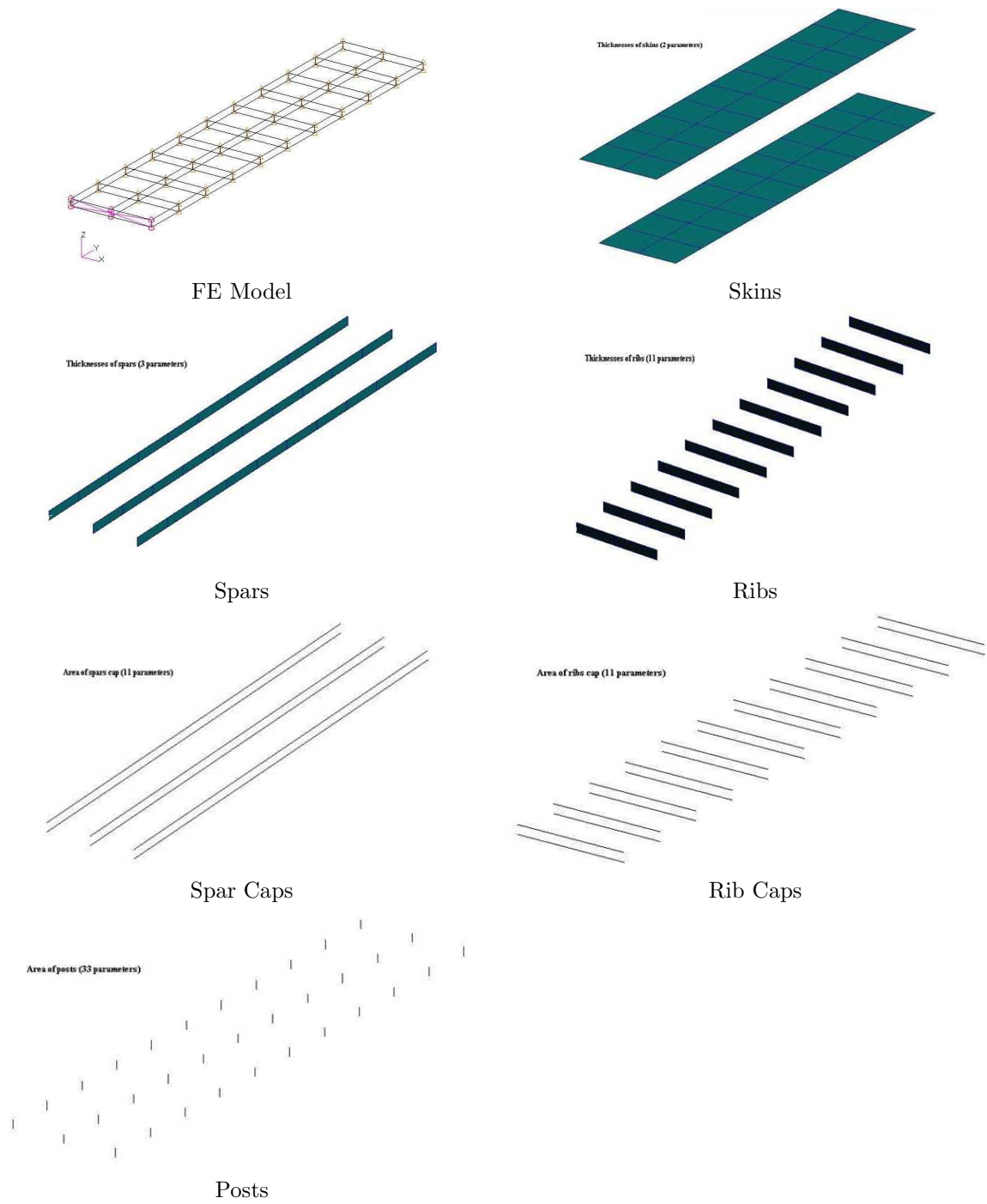
Figure 2. Views of the structural model for the clean Goland wing.

American Institute of Aeronautics and Astronautics
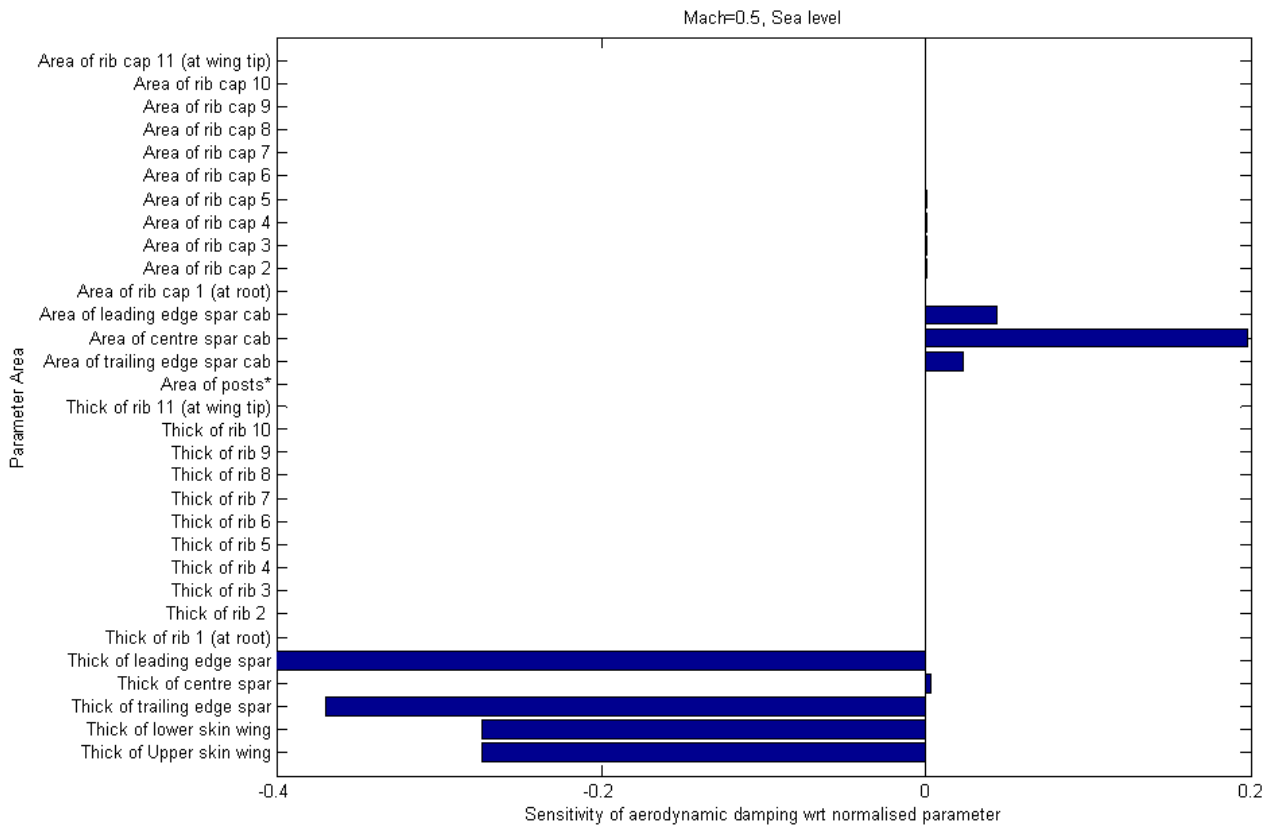
Figure 3. Sensitivity with respect to the structural parameters of the clean wing Aeroelastic Damping at Mach 0.5 and sea level computed using linear analysis[22] for the clean Goland Wing.

American Institute of Aeronautics and Astronautics

used to allow the feasibility (from a computational cost viewpoint) of the evaluation of the sensitivity of the flutter speed to structural parameters to be made.

The seven identified structural parameters were randomised by taking a coefficient of variation of 0.05 about the mean value, and a set of 1000 normal modes was generated. The Schur matrix was calculated at the mean parameter values, at a cost of 64 linear solves, and this matrix was then used to drive convergence of the quasi-Newton method for all the other random parameter combinations. The four aeroelastic eigenvalues were then computed for the 1000 samples. In each case the eigenvalues converged in 3-4 quasi-Newton steps, meaning that the computational cost at each altitude was 3-4 linear solves.

The linear perturbation method requires the calculation of the Jacobian of the aeroelastic eigenvalue with respect to each of the seven uncertain structural parameters at each altitude of interest, requiring 3-4 linear solves per parameter per altitude.

Finally, for the interval method the first step is to calculate the mean parameter aeroelastic eigenvalues. The eigenvalues which are close to becoming undamped and the range of critical altitude for these eigenvalues are selected. The interval analysis optimisation is then run at these altitudes and for these eigenvalues. The Schur matrix is re-evaluated at the mean value for each altitude chosen to drive rapid convergence for each function evaluation during the optimisation. It was found that in the worst case around 12 optimisation steps was required to achieve convergence to the maximum or minimum eigenvalue real part, needing 96 eigenvalue calculations. In total this took around 4 hours of CPU time in the worst case to define both ends of the range. For the maximum possible value for the real part of the eigenvalue the structural parameters converge to one or other end of the parameter interval, as indicated in table 1 where the uncertain parameters have been scaled onto the interval [-1,1]. For the minimum possible value (which is of less interest), some parameter values converge to internal values.

Parameter	Upper wing skin	Lower wing skin	LE Spar	TE Spar	LE Spar Cap	Centre Spar Cap	TE Spar Cap
10000ft	-1.0	-1.0	-1.0	-1.0	1.0	1.0	1.0
9000ft	-1.0	-1.0	-1.0	-1.0	1.0	1.0	1.0
2000ft	-1.0	-1.0	-1.0	-1.0	1.0	1.0	1.0

Table 1. Converged structural parameter values for the maximum real part at different altitudes. Note that the optimum is for the parameter scaled onto an interval [-1,1]. The results are for the Goland Wing Clean Case.

The mode tracking, together with the influence of structural variability, is shown in figure 4. In this figure the lines indicate the eigenvalues predicted using the series approximation to the residual of equation 7 whereas the points are from a full evaluation at that altitude. The two sets of results are in perfect agreement for this case, suggesting that the series approximation is good. On parts (a) and (b) of this figure the mean parameter mode tracking is shown. The interaction of the first wing bending and torsion modes is clear in figure 4(b) with the convergence of frequencies below 10000 ft. The bending mode becomes undamped, as shown in figure 4(a). The influence of structural variability is shown at three altitudes in figure 4(c). This figure includes the Monte-Carlo simulation results (with each sample indicated by one point on the graph), the perturbation results (with the 2σ results indicated by circles) and the interval maximum and minimum indicated by the lines. The first observation is that the scatter of the results on the real part of the eigenvalue is very small before the modes start to interact strongly. After this interaction starts the spread of results grows dramatically. The interval results capture the Monte-Carlo samples, as they should. The probability distribution functions (pdf) from the Monte-Carlo and perturbation methods are shown in figure 5. There is a kink in the distribution on the stable side of the real part of the eigenvalue at 9000 ft where the interaction is starting. The most significant discrepancy compared with the perturbation generated distribution is in the tail on the unstable side. On the more unstable side at 2000 ft the perturbation distribution is almost identical with that derived from the Monte Carlo distribution.

Interval calculations at a number of altitudes allow lower and upper interval bounds to be traced as a function of altitude. These curves are shown in figure 6 which shows that the altitude range for flutter onset is from 14000 ft down to 5000 ft.
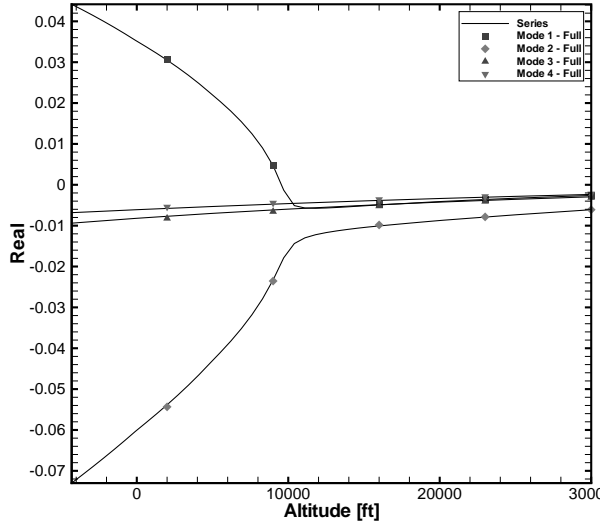
American Institute of Aeronautics and Astronautics

(a) Mean Eigenvalues - Real Part
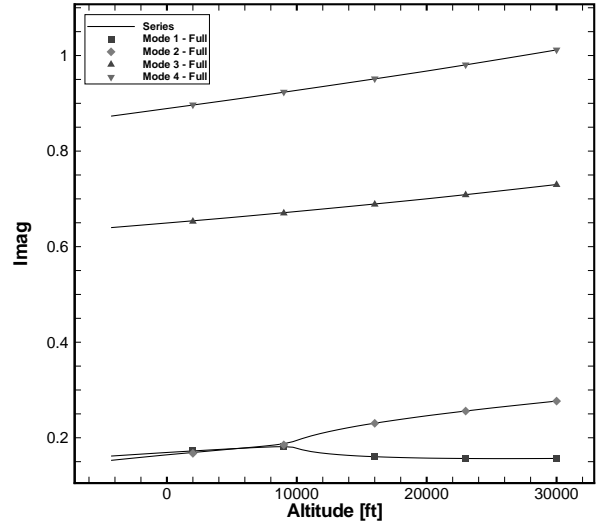
(b) Mean Eigenvalues - Imaginary Part
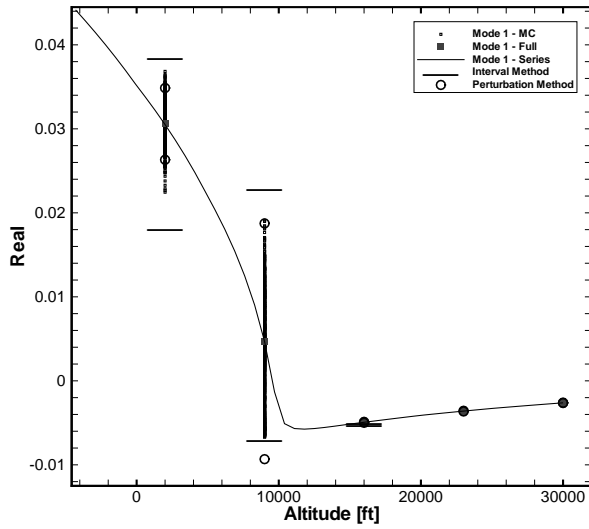
(c) Variability on Mode 1 Eigenvalue Real Part

Figure 4. Goland Wing Clean Configuration Mode tracking, including the influence of structural variability. MC refers to Monte Carlo and the circles on the figure are the 2σ values from the perturbation pdf.

American Institute of Aeronautics and Astronautics

9000ft   2000ft
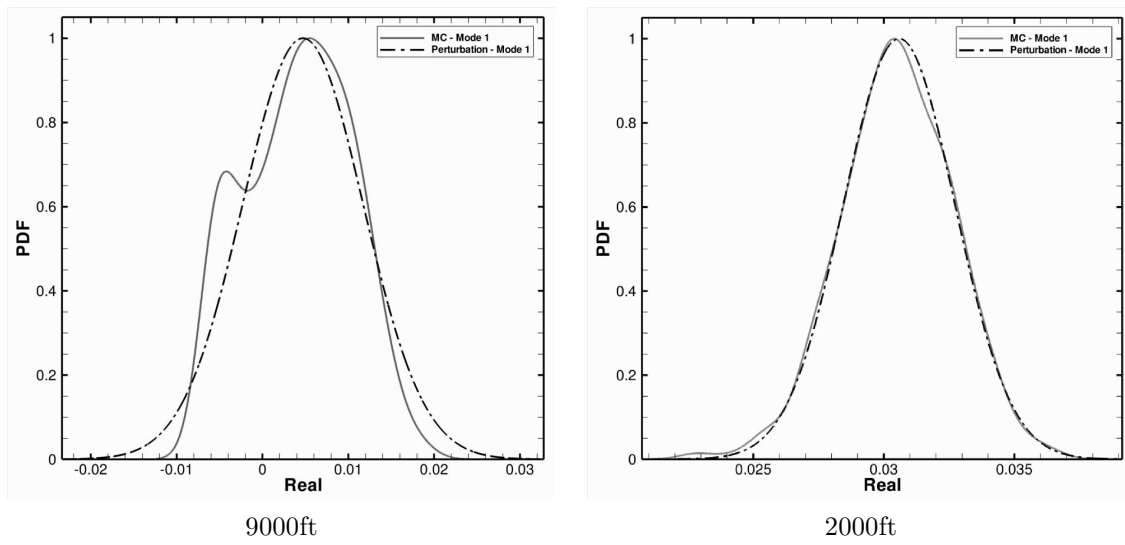
Figure 5. Probability Density Functions - Goland Wing Clean Case
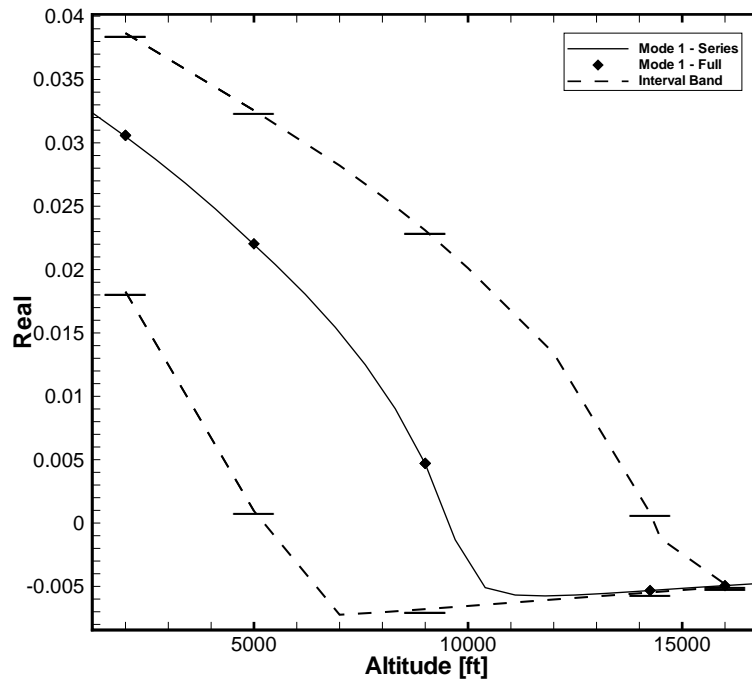
Figure 6. Range of flutter speed from Interval Analysis for Goland Wing Clean Case.

American Institute of Aeronautics and Astronautics

The costs of the different approaches is shown in table 2. These costs are shown both in terms of the number of eigenvalue calculations and also the CPU time on a Pentium 3GHz processor (i.e. a desktop computer). The linear perturbation method has a small cost, but cannot capture skewness in the pdf if this is present. The interval method requires up to 4 hours to define the worst case interval. Finally, even the Monte-Carlo simulation only requires 50 hours for 1000 samples.

Given that the amount of variability in the structural parameters is likely to be based on the intuition of an analyst rather than on hard statistical data, the essential information in the results of these analyses is in the spread of the results rather than in the pdf. If this is accepted then the interval results have a good balance between capturing the spread (including any skewness) and the computational cost, and it will be used for the remaining cases in this paper.

Method	Number of eigenvalue evaluations	Wall Clock Time
Monte Carlo	1000	50h
Perturbation	7	21min
Interval	60 - 190	2.5 - 8h
Single Flutter Point	1	3min

Table 2. Comparison of methods to calculate the eigenvalue real part variability for the critical mode at one altitude

.

C. Tip Store Results

The case with a tip store is interesting because there is a Mach number range above 0.92 which features a rapid reduction in stability, and the appearance of limit cycle oscillations. An important contribution to this behaviour comes from the development of a strong shock wave. The flutter boundary in terms of the critical altitude as a function of Mach number is shown in figure 7. The rapid loss of stability is indicated by the boundary heading vertically up on the figure at Mach 0.92. The critical mode switches around this Mach number from the first (mode 1) to the second (mode 3) bending, as annotated on the figure. The same structural variation is applied as for the clean wing. The intervals on the flutter altitude are included in figure 7. Also include on the figure is the mean parameter prediction from the linear analysis NASTRAN. The main difference with the CFD based results comes around values of Mach number of 0.92 where the shock is destabilising, an effect not seen by the linear predictions. Also, the uncertain interval for the linear results is included at Mach 0.7 and is very similar in extent to the CFD based interval at this Mach number. The modal interaction results at Mach 0.9 are shown in figure 8. Throughout the Mach number range the first mode is lightly damped, and the structural variability creates a significant variation on the flutter altitude, as illustrated in figures 8(c) and 8(d). It is however interesting to note that the variation in the flutter altitude does not increase as the Mach number approaches the critical value (0.92) where the stability is rapidly lost due to aerodynamic effects.

D. Generic Fighter Model

Having demonstrated the approach to evaluating sensitivity on a model wing, a second case is computed to show feasibility on a realistically sized aircraft model. The intention here is to show that the method can scale to models of the size required for the analysis of aircraft. The generic fighter was built on data publically available for the F-16 aircraft, since this has been the subject of much interest from an aeroelastic viewpoint. The approach was to establish a test case which is recognisable as an aircraft, but which obviously cannot replicate the actual behaviour of the F-16. In order to study store induced effects,[23] a model with similar aerodynamic and structural characteristics to the F-16 was built. Available data of the wing geometry (dimensions and aerofoil section), together with published data from Ground Vibration Tests (GVT) and wind-tunnel data was exploited.

American Institute of Aeronautics and Astronautics
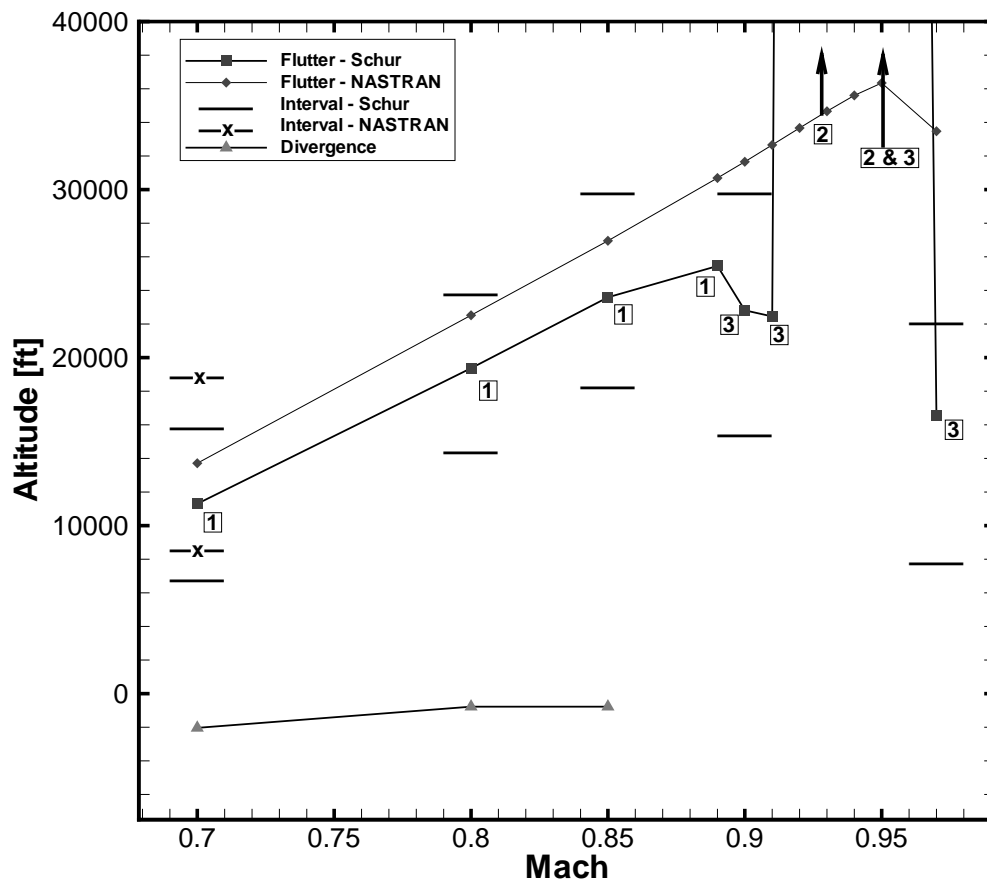
Figure 7. Instability boundary - Goland Wing Store Case
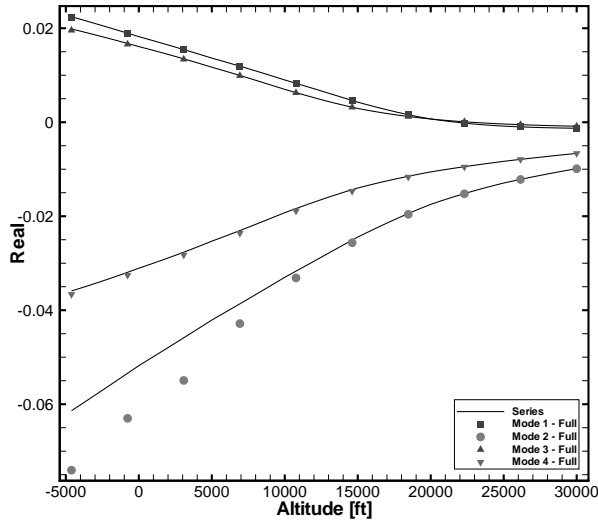
(a) Mean Eigenvalues - Real Part
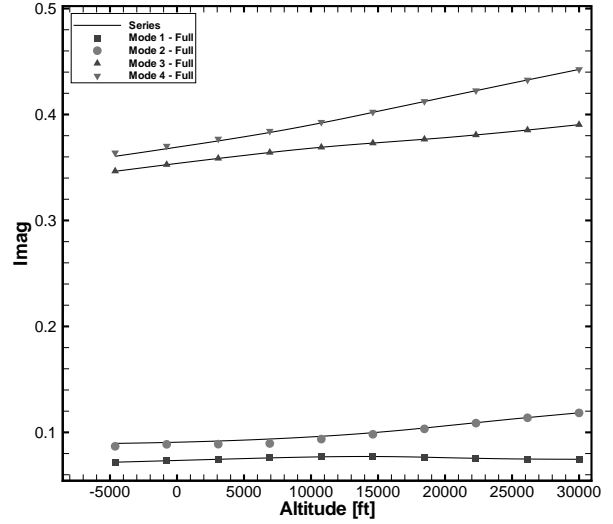
(b) Mean Eigenvalues - Imaginary Part
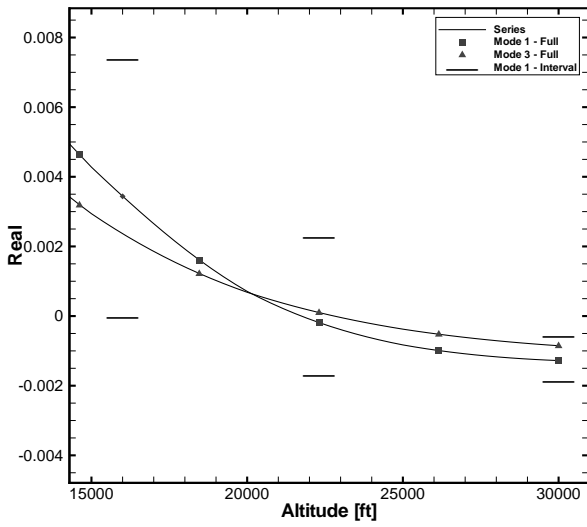
(c) Variability on Mode 1 Eigenvalue - Real Part
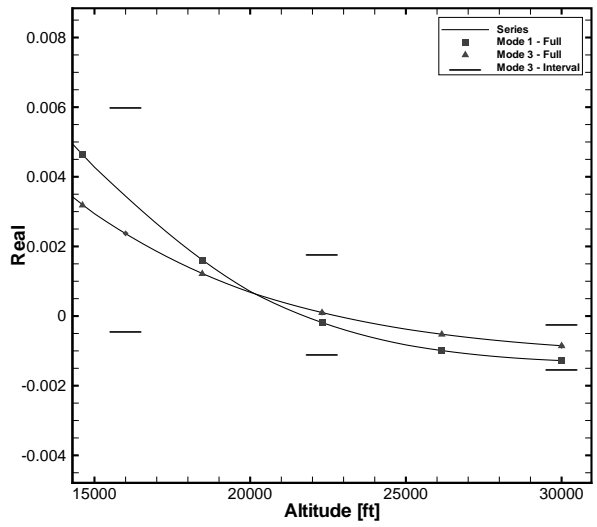
(c) Variability on Mode 3 Eigenvalue - Real Part

Figure 8. Eigenvalue variation with altitude at Mach 0.9 - Goland Wing Store Case

The geometry is summarised in figure 9 and is an extension of that described in reference.[10] The basic shape of this model started from an artistic CAD model of the F-16. The model has several inaccuracies with respect to the fuselage geometry, however it is thought that a reasonable first generic test case for store induced aeroelastic behaviour can be obtained without the exact fuselage and tail aerodynamics initially. Hence, in the first version of the model the tail plane has been removed. The aerofoil section consists of a NACA 64A204 profile, with a wing root angle of $-1°$ and a wing tip angle of $-2.4°$. The wing twist was chosen by comparing surface pressures against results given in ref.,[24] which include CFD studies based on the real geometry of the F-16 and wind-tunnel measurements; this test case corresponds to a free stream Mach number of 0.85 at an angle of attack of $2.12°$. The un-twisted wing developed a shock wave at the wing tip junction with the tip rail. To mitigate these effects, the effective angle of attack was reduced by adding negative twist at the wing tip. The upper and lower surfaces were then generated by sweeping the tip aerofoil up to the wing root. A few iterations were necessary to obtain the final configuration.

From the definition of the geometry, a H-Type block structured grid was used around the wing and a C-Type block topology was applied around the fuselage. The grid has 1.06 million points and 344 blocks for the full configuration. The surface grid is shown in figure 9 and shows that the points are concentrated on the wing which contributes most to the aeroelastic response in this test case. Figure 10 shows the comparison with wind tunnel measurements of the surface pressures at two locations along the span. The untwisted wing solution is included for comparison.

The finite-element (FE) model of the wing was built based on the model proposed by Cattarius[25] and is shown in figure 11. The structural model consists of four parts: fuselage, wing, pylon and stores. The fuselage was modelled by using QUAD4 elements with the properties indicated in table 3. The fuselage is modelled to behave as a rigid body. The pylon and stores were also modelled by using QUAD4 elements and properties are given in table 3. Lump mass elements were used to model the mass properties of both pylon and stores. The triangular elements, shown in figure 11, indicate a lump mass element. Table 4 shows mass properties of the pylon and store. The pylon is rigidly connected to the wing. The store is connected to the pylon by six spring elements (three translational and three rotational). The wing is also modelled using shell elements (QUAD4) and is divided into three regions: root, pylon, and tip.

In order to match the natural frequencies of the FE model to those found in the Ground Vibration Test,[26] the Young's modulus and density of each region of the wing are considered as updating parameters. Table 6 shows the first five symmetric natural frequencies of the updated FE model and GVT data. Updated properties of the wing are given in table 5. Figure 12 shows the first eight mode shapes of full model of wing including both symmetric and anti-symmetric modes.

Property	
E $[GPa]$	115
G $[GPa]$	46
$\rho\ [kg/m^3]$	1
ν	0.25
t $[m]$	0.001

Table 3. Fuselage, pylon and stores rigid shell element properties for Generic Fighter.

A linear sensitivity analysis for the flutter speed against the structural parameters was again carried out using NASTRAN.[22] This identified that the most important structural parameters were the rotational spring coefficient for the store attachment, the Young's modulus of the wing root section and the pylon, and the densities for the wing root and tip regions and the pylon. An interval of was defined for each of these parameters as plus and minus 30% for the rotational spring coefficient and 10% for the other parameters.

The Schur flutter analysis for the mean and varying structural paranmeters is shown in figure 13. On parts (a) and (b) the real and imaginary parts at the mean structural parameters are shown respectively for all modes. The asymmetric second and third modes

American Institute of Aeronautics and Astronautics

Tip: NACA64$_A$204 Section
set at -2.4° to horizontal

1.134m

3.572m

3.846m

14.472m

2.589m

Root: NACA64$_A$204 Section
set at -1.0° to horizontal
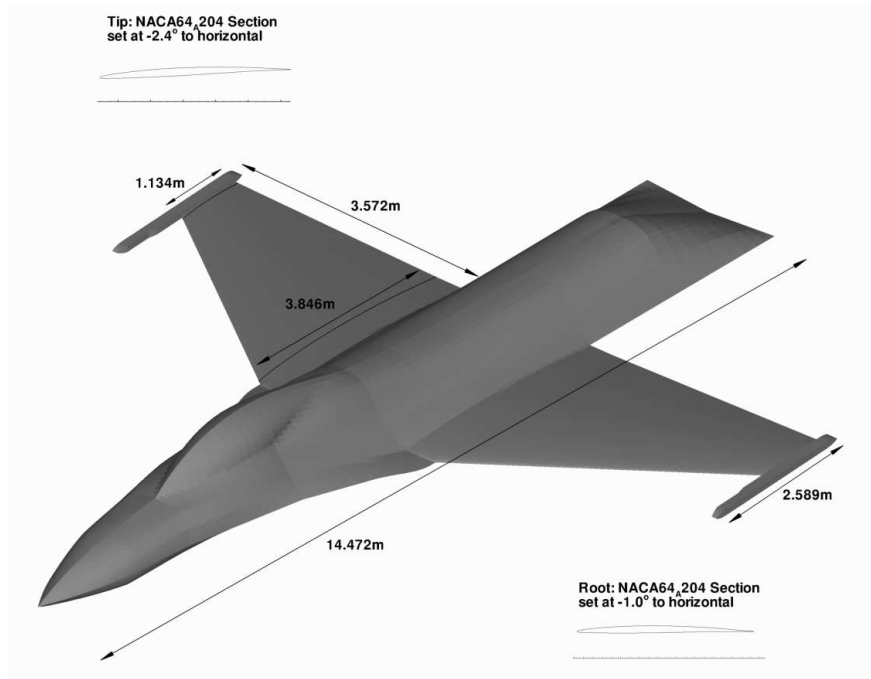
Summary of Geometry
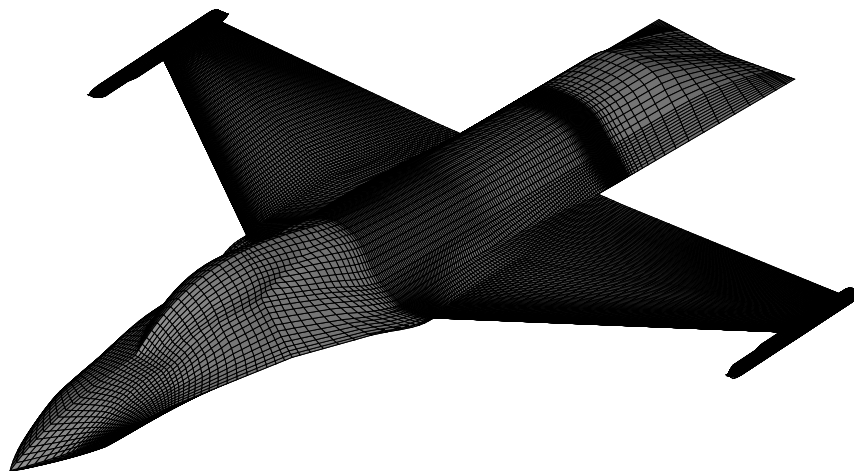
CFD surface grid

Figure 9. Generic fighter geometry and surface CFD and FEM grids.

American Institute of Aeronautics and Astronautics

(a) 59% Span   (b) 85% Span
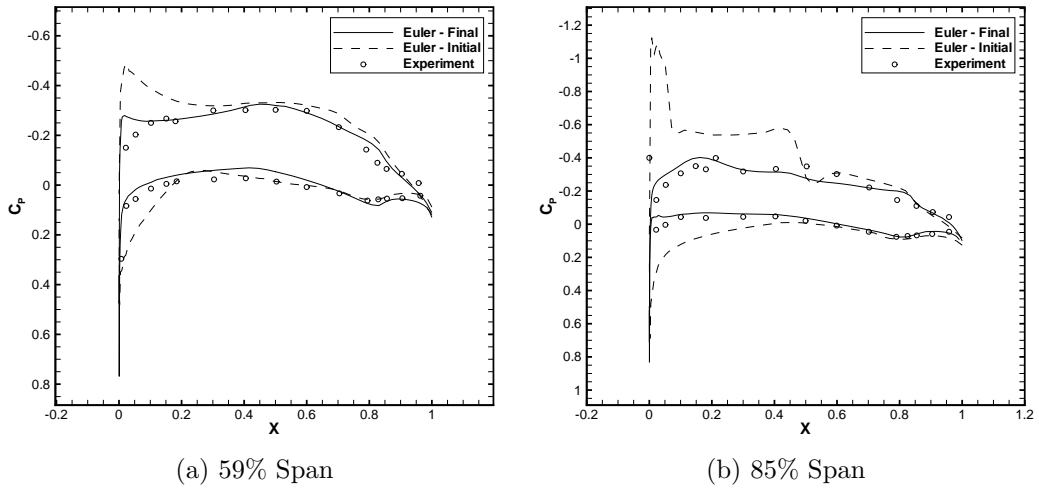
Figure 10. Surface pressure comparison for Mock Fighter: $M = 0.85$, $\alpha = 2.12°$
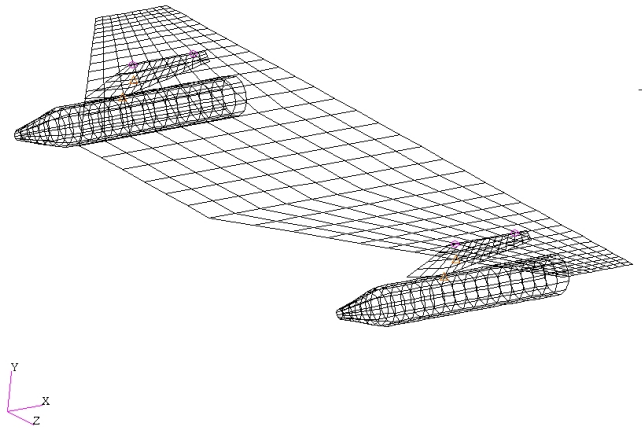
Figure 11. Structural Finite Element Model for the Generic Fighter.

American Institute of Aeronautics and Astronautics

3.74Hz

4.48Hz

5.03Hz

5.92Hz

7.99Hz

8.12Hz

11.00Hz

11.39Hz
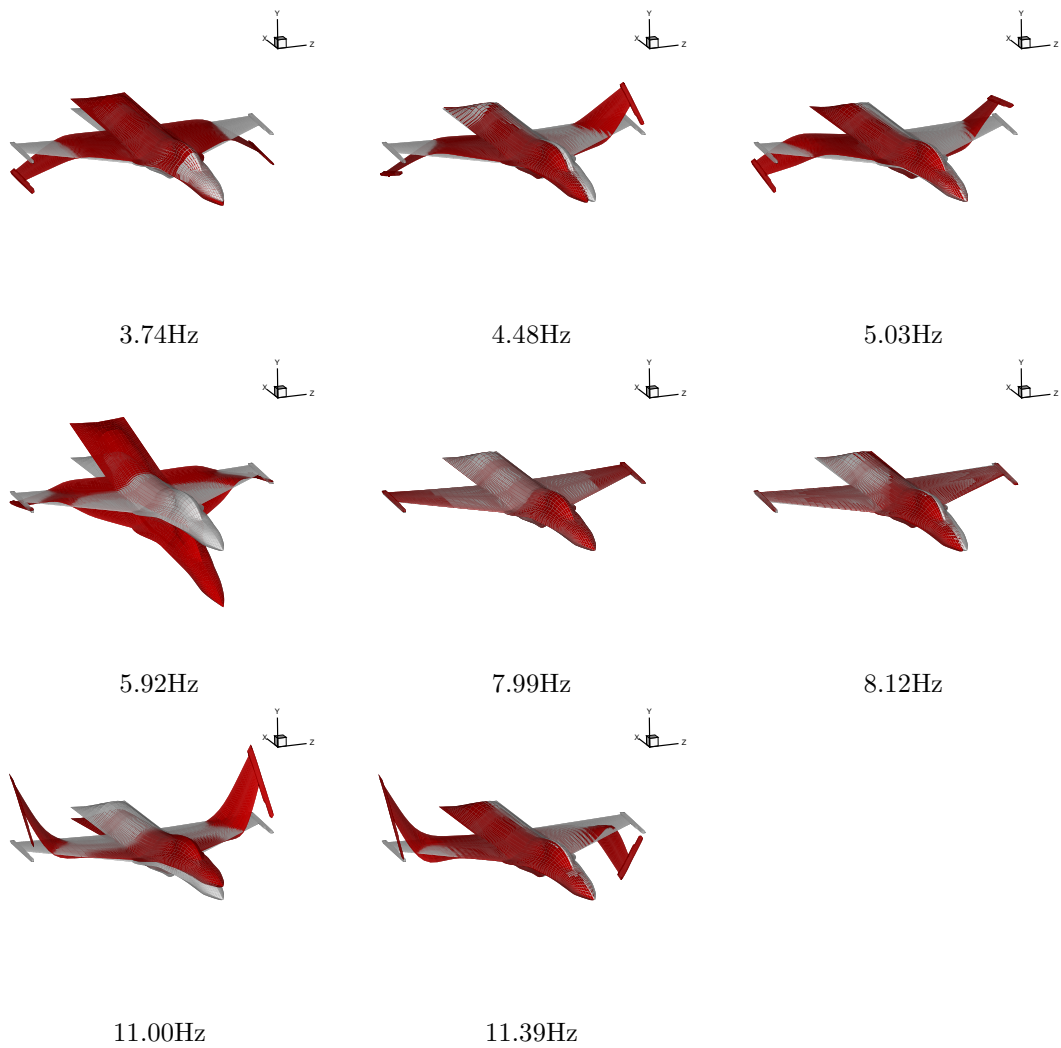
Figure 12. Mapped Structural Normal Modes for the Generic Fighter.
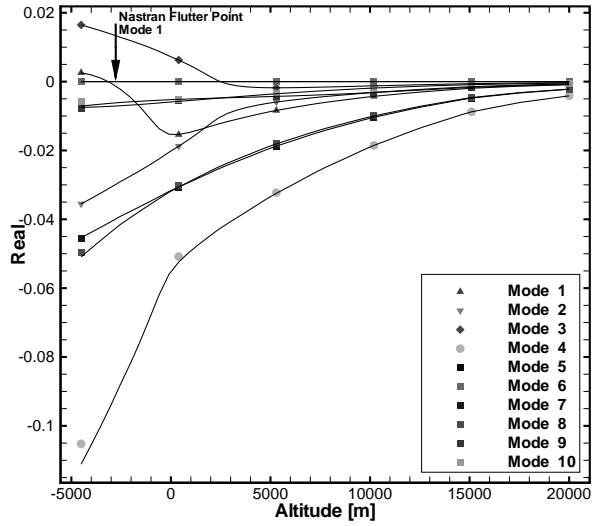
American Institute of Aeronautics and Astronautics

(a) Mean Eigenvalues - Real Part
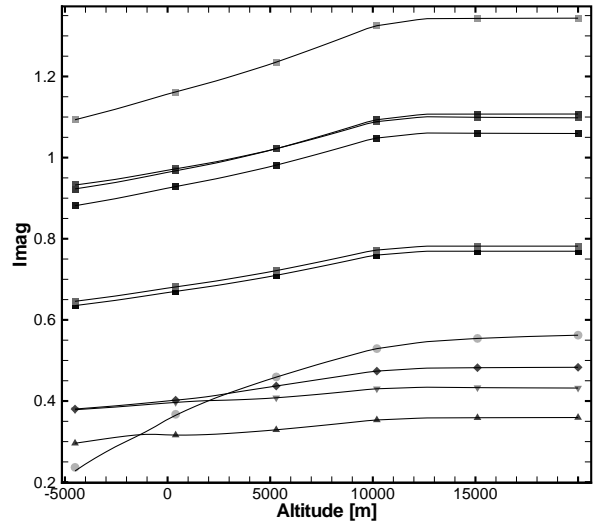
(b) Mean Eigenvalues - Imaginary Part
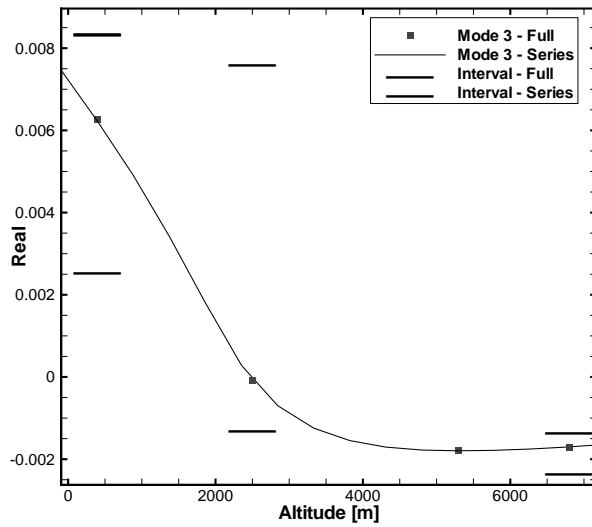
(c) Variability on Mode 3 Eigenvalue - Real Part
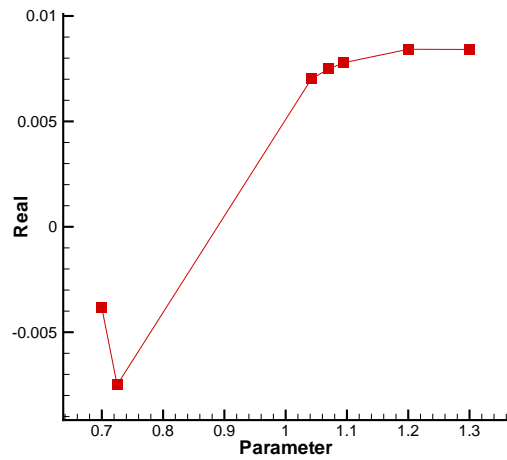
(d) Mode 3 Real Part with rotational spring coefficient

Figure 13. Eigenvalue variation with altitude at Mach 0.85 - Mock Fighter Case

Property	Pylon	Store
Mass $[kg]$	161	1027.5
$\mathrm{I}_{xx}\ [kg \cdot m^2]$	–	27.5
$\mathrm{I}_{yy}\ [kg \cdot m^2]$	–	1000
$\mathrm{I}_{zz}\ [kg \cdot m^2]$	–	1000

Table 4. Mass properties of pylon and stores for Generic Fighter.

Property	Root	Pylon	Tip
E $[GPa]$	157.3	96.7	95.6
G $[GPa]$	62.9	38.7	38.2
$\rho\ [kg/m^3]$	5680	3780	3780
ν	0.25	0.25	0.25
t $[m]$	0.075	0.03	0.03

Table 5. Wing rigid shell element properties for Generic Fighter.

interact, with the third mode going undamped at about 2000m. The series and full predictions are in good agreement.

The intervals for mode 3 at 6750 and 2500m are shown in part (c) of the figure. Similar behaviour to the Goland wing is observed i.e. the interval grows significantly after the modal interaction becomes strong. Again the mean parameter matrices were used to drive convergence of the Schur calculations during the optimisation. This was done on 44 processors of a PC cluster and took around 7 hours at the higher altitude. The structural variation chosen was high in this case and the mean matrices were not sufficient to drive convergence for some parameter values at the lower altitude. If Newton convergence is not observed then the iterations are stopped, the Schur matrices regenerated and the iterations restarted. All of the parameters except the rotational spring coefficient of the spring attachment converged to one end of their range with a few optimisation steps. However, the spring coefficient parameter exhibited slow covergence. The values of the other parameters were fixed at the extreme which they settled to during the optimisation, and the real eigenvalue was traced as a function of the spring parameter and this is shown in figure 13(d). Note that the parameter value has been normalised onto an interval [0.7:1.3] which indicates the scaling of the original spring parameter. The maximum real part was attained at a value of 1.2 and the flat distribution at the top end of the interval is noted, perhaps explaining the slow convergence of the optimiser.

VI.   Conclusions

The feasibility of using three methods to propagate structural model variability to aeroelastic stability prediction has been investigated. The methods considered were Monte-Carlo simulation, perturbation analysis and interval analysis. The feasibility in terms of computational cost was demonstrated, when using CFD, by exploiting an eigenvalue based method which can be configured for the purpose of computing stability for many similar structural models. A rapid increase in the sensitivity of the real part of the critical eigenvalue to the structural variability was observed after the modal interaction starts. Two test cases were considered, the first based on the Goland wing and the second on a generic fighter. The most important structural parameters for flutter were determined through a linear sensitivity analysis, and in this way O(10) parameters were chosen for the variability analysis. For the Goland wing, 1000 structural samples were computed in two days on a desktop PC, and the interval results in around 3 hours.

An interesting question is how to use these methods for applications. The generation of probability distributions by Monte Carlo analysis and perturbation analysis is attractive for certification applications, but this attraction may be deceptive. These distributions

American Institute of Aeronautics and Astronautics

	Mode 1	Mode 2	Mode 3	Mode 4	Mode 5
Updated FE model	3.74 h_1	5.91 $\alpha + \theta$	8.12 γ	11.0 $h_2 + \alpha$	11.51 $\theta_{\alpha,\ T}$
GVT[26]	4.07 h_1	5.35 $\alpha + \theta$	8.12 γ	12.25 h_2	

h_i - i^{th} bending; α - pitch; θ - torsion; γ - yaw; $\theta_{\alpha,\ T}$ - tip torsion+pitch

Table 6. Symmetric mode frequencies for Generic Fighter.

must be interpreted in the light of the definition of the structural variation distributions. These are likely to be based on the best guess of the analyst since hard data is unlikely to be available. In these circumstances the important information is in the spread of the eigenvalue real parts. The interval method captures this spread, and also skewness about the mean, in a reasonable computational cost. This method is therefore favoured based on this consideration.

VII.   Acknowledgements

References

[1]Pettit, C., Uncertainty Quantification in Aeroelasticity: Recent Results and Research Challenges, Journal of Aircraft, 41(5), 1217-1229, 2004.

[2]Walters, R., Huyse, L., Uncertainty Analysis for Fluid Mechanics with Applications, Tech. Rept. NASA/CR 2002-211449, Feb. 2002

[3]Pitt, D., Haudrich, P.,Thomas, M., Probabilistic Aeroelastic Analysis and Its Implications on Flutter Margin Requirements. AIAA-2008-2198 in the proceedings of 49th AIAA/ASME/ASCE/AHS/ASC Structures, Structural Dynamics and Materials Conference, AIAA, Schaumburg, Illinois (2008).

[4]Ghanem, R., Spanos, P., Stochastic Finite Elements: A Spectral Approach, Dover Publications Inc., Revised Edition, 2003

[5]Majumder, L., Rao, S., Interval-based optimization of aircraft wings under landing loads, Computers and Structures (87), 225235, 2009

[6]Kurdi M, Lindsley N and Beran P, Uncertainty quantification of the Goland wing's flutter boundary, AIAA Paper 2007-6309, August 20-22.

[7]Willcox, K. Peraire, J., Application of Reduced-Order Aerodynamic Modeling to the Analysis of Structural Uncertainty in Bladed Disks, Proceedings of ASME TURBO EXPO 2002 International Gas Turbine & Aeroengine Congress & Exhibition, Amsterdam, The Netherlands, June 3-6, 2002

[8]Verhoosel C., Scholcz, T., Hulshoff, S., Gutiérrez M., Uncertainty and Reliability Analysis of Fluid-Structure Stability Boundaries, AIAA Journal, 47(1), 91-102, 2009

[9]Rao, S., Majumder, L., Optimization of Aircraft Wings for Gust Loads: Interval Analysis-Based Approach, AIAA Journal 46(3), 723732, 2008

[10]Badcock, K.J. and Woodgate, M.A., Prediction of Bifurcation Onset of Large Order Aeroelastic Models, 49th Structural Dynamics and Materials Conference, Schaumberg, Illinois, May, 2008, AIAA-2008-1820.

[11]Badcock, K.J., M.A. Woodgate, M.A. and Richards, B.E., The Application of Sparse Matrix Techniques for the CFD based Aeroelastic Bifurcation Analysis of a Symmetric Aerofoil, AIAA Journal, 42(5), 883-892, May, 2004.

[12]Badcock, K.J., Woodgate, M.A. and Richards, B.E., Direct Aeroelastic Bifurcation Analysis of a Symmetric Wing Based on the Euler Equations, Journal of Aircraft, 42(3),731-737, 2005.

[13]Bekas, K. and Saad, Y., Computation of Smallest Eigenvalues using Spectral Schur Complements, SIAM Journal of Scientific Computing, 27(2), 2005, 458-481.

[14]Bowman, A. W., and A. Azzalini, Applied Smoothing Techniques for Data Analysis, Oxford University Press,1997.

[15]Mathai A.M., and Provost, S.B., Quadratic Forms in Random Variables: Theory and Applications. Marcel Dekker, New York, NY, 1992.

[16]Kapur JN, Kesavan HK. Entropy Optimization Principles With Applications. Academic Press: San Diego, CA, 1992.

[17]Adhikari S. and Friswell M, Random matrix eigenvalue problems in structural dynamics. International journal for Numerical Methods in Engineering, 69, 2007, 562-591.

[18]Gill, P.E., W. Murray, and M.H. Wright, Practical Optimization, London, Academic Press, 1981.

[19]Han, S. P., A Globally Convergent Method for Nonlinear Programming, Journal of Optimiza-

American Institute of Aeronautics and Astronautics

tion Theory and Applications, vol. 22, p.297, 1977.

[20]Powell, M. D., A Fast Algorithm for Nonlinearly Constrained Optimization Calculations, Numerical Analysis, ed. G.A. Watson, Lecture Notes in Mathematics, Springer Verlag, Vol. 630, 1978.

[21]Beran, P.S., Knot, N.S., Eastep, F.E., Synder, R.D. and Zweber, J.V., Numerical Analysis of Store-Induced Limit Cycle Oscillarion, Journal of Aircraft, 41(6), 1315-1326, 2004.

[22]Khodaparast,H.H., Mottershead, J.E. and Badcock, K.J., Propagation of Structural Uncertainty to Linear Aeroelastic Stability, in review in Computers and Fluids.

[23]Denegri, C., Limit Cycle Oscillation Flight Test Results of a Fighter with External Stores, Journal of Aircraft, 37(5), 761-769, 2000.

[24]Denegri, C., Dubben, J., F-16 Limit Cycle Oscillation Analysis Using Transonic Small-disturbance Theory. In: AIAA-2005-2296 - 46th AIAA/ASME/ASCE/AHS/ASC Structures, Structural Dynamics and Materials Conference, AIAA, Austin, Texas (2005).

[25]Cattarius, J,Numerical Wing/Store Interaction Analysis of a Parametric F-16 Wing,PhD Thesis, Virginia Polytechnic Institute and State University, Blacksburg, Virginia, U.S., 1999.

[26]Cazier, F.W. Jr and Keloe, M.W., Ground Vibration Test on an F-16 airplane with modified decoupler pylons. Technical Memorandum NASA-TM-87634, NASA, 1986.